PHYSICAL REVIEW B **78**, 121408(R) (2008)

Interplay between adsorbate-induced reconstruction and local strain: Formation of phases on the Cu(110)-(2×1):O surface

Kirill Bobrov and Laurent Guillemot
CNRS, UMR 8625, Laboratoire des Collisions Atomiques et Moléculaires, LCAM, Bâtiment 351, UPS-11, Orsay F-91405, France and Université Paris-Sud, Orsay F-91405, France

(Received 14 May 2008; revised manuscript received 15 July 2008; published 25 September 2008)

We present an STM study on the interplay between adsorbate-induced reconstruction and local strain on the oxygen adsorbed Cu(110) surface. Thermal annealing of the surface resulted in surface terrace ripening revealing larger terraces, uniformly covered by the (2×1)-O reconstructed phase, separated by step bunches. The largest terrace was found to be partially splitted by emerging dislocations inducing strong inhomogeneous strain in their close vicinity. This extra strain caused local conversion of the dominating (2×1)-O phase into oxygen chemisorbed phases drastically different from the dominating phase. A meaningful correlation between lateral evolution of the extra strain and structure of these phases has been found. The symmetry of the discovered phases has been determined and their structural models have been elaborated.

DOI: 10.1103/PhysRevB.78.121408 PACS number(s): 68.35.Gy, 68.37.Ef, 68.43.Fg, 68.43.Hn

The relationship between adsorbate-induced surface strain and surface reconstruction phenomena has been extensively studied in the past last years. Ibach[1] has demonstrated that adsorbates generally modified the intrinsic tensile strain of metal surfaces as a result of adsorbate-surface charge transfer that always occurs upon chemisorption. The chemisorption of carbon on the Ni(100) surface[2] represents an excellent example of the correlation between surface strain and reconstruction phenomena. The dynamical equilibrium between the coexisting $p(2\times2)$-C and (2×2)-C $p4g$ phases is established due to a balance between the energy gain, associated with the stronger chemical bonding in the reconstructed (2×2) $p4g$ phase, and the energy cost associated with the conversion of the nonreconstructed $p(2\times2)$ phase into the strained (2×2) $p4g$ configuration. The general question which immediately arises from analysis of this example is whether extra surface strain can alter the energetic of an adsorbate-substrate interface and, therefore, modify the state of chemisorbed particles. If true, extra strain introduced into a surface in a controlled manner can serve as a nanofabrication tool,[3] which is supposed to modify the surface reactivity[4] and to fabricate particularly reconstructed phases. However, quantitative and reliable evaluation of the role of extra strain in modification of adsorbate structures represents a challenge. Macroscopically applied external stress will lead to formation of bulk dislocations which form easily in metals and release the strain. The residual surface lattice deformation is limited to few tenths of a percent that will unlikely result in measurable modification of an adsorption phase. Substantially larger macroscopic strain could be produced in thin pseudomorphical heteroepitaxial films grown on lattice mismatched substrates. Here, however, the film thickness is limited to a few monolayers (in thicker films strain is relieved by creation of a surface dislocation network). Adsorbates on such a strained surface will be influenced by the strain of the film lattice as well as the electronic structure of the nearby substrate.[5] Discrimination of these effects is possible only in limited number of cases that required detailed *ab initio* calculations of film-substrate interface structure[6,7] and strain relaxation within a film.[8] Alternative way to evaluate the role of the extra strain is to introduce local stress on a surface by an external influence. Gsell *et al.*[9] have observed that local strain on the Ru(0001)/O surface, introduced by Ar implantation into near-surface region, caused segregation of chemisorbed oxygen onto the areas stretched locally by underlying implanted Ar bubbles. However, no changes in the oxygen adsorbate structure have been detected probably due to a weakness of the strain field associated with only slight local deformation (0.2%) of the Ru(0001) lattice.

In this Rapid Communication, we present the first experimental evidence that extra strain, introduced into a surface locally, can directly modify adsorbate structure and fabricate particularly reconstructed phases. Specifically, we will show that extra strain introduced into the Cu(110)-(2×1)-O surface made the dominating (2×1)-O phase locally unstable, favoring its transformation in drastically different reconstructed phases. In order to introduce extra strain into the surface we will exploit the natural instability of vicinal Cu(11n) with $n=3$, 5, and 9 surfaces against oxygen-induced faceting.[10] On the Cu(110) surface this instability is manifested by terrace ripening, driven locally by the (2×1)-O phase formation at elevated temperatures and favoring larger terraces.[11,12] This process will certainly introduce strain into the surface since the progressively growing atomically flat terraces must accommodate corrugated morphology of the underlying substrate induced by slight macroscopic sample miscut.[13]

In order to prepare the well-ordered Cu(110)-(2×1):O surface[14] we used the following procedure. A single-crystal Cu(110) sample cut with maximal achievable accuracy of ~0.1° was used in this study. The thoroughly polished Cu(110) sample was cleaned *in situ* by repeated cycles of sputtering (1 keV Ar^+) at grazing incident angles followed by thermal annealing at 600 °C. Molecular oxygen adsorption was performed at ~220 °C by *in situ* exposing the Cu(110) surface to oxygen at $P=5\times10^{-10}$ mbar for ~15 min until ~0.25 ML oxygen coverage was reached on the surface. Cleanness of the prepared surface was controlled by Auger electron spectroscopy (AES) and scanning tunneling microscope (STM), no impurities were detected. The surface was

 ©2008 The American Physical Society

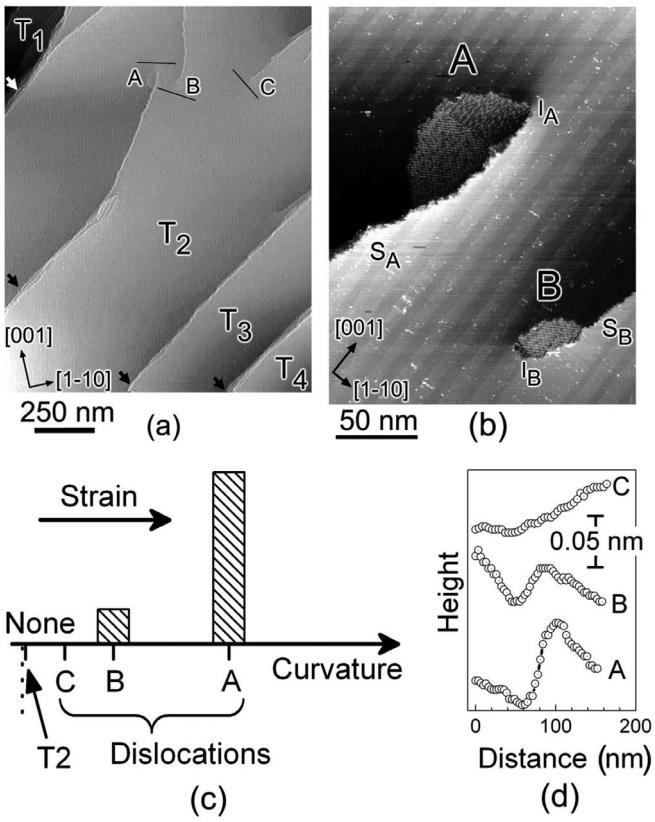

FIG. 1. Formation of reconstructed phases on the annealed Cu(110)-(2×1)-O surface. (a) STM topography (U_{bias}=−1.2 V, I_t=0.5 nA) of the Cu(110)-(2×1)-O surface annealed at 500 °C for 30 min. The step bunches separating the terraces (T_1-T_4) are marked by arrows. The surface dislocations are denoted as *A*, *B*, and *C*. The black lines depict STM height profiles taken in vicinity of the dislocations. (b) STM topography of the surface area around the *A* and *B* dislocations. The (2×1)-O strips running in [001] direction are clearly visible. The dislocation-induced surface steps and the corresponding splitting points are denoted as S_A, S_B, and I_A, I_B, respectively. (c) The area of the phases (hatched bars) as a function of the surface curvature in vicinity of the *A*, *B*, and *C* dislocations. The curvature of the T_2 terrace and the zero curvature of a flat surface (dotted line) are indicated for comparison. (d) STM height profiles used in (c) to determine the surface curvatures.

then annealed at 500 °C, cooled down to room temperature (RT) and STM topographies were recorded in constant current mode.

Figure 1(a) shows the STM topography of the Cu(110)-(2×1)-O surface. The thermally induced terrace ripening revealed large surface terraces (T_1-T_4) separated by step bunches. The accommodation of the largest T_2 terrace to the mesoscopic variation of the sample miscut angle revealed its partial splitting. Smaller terraces separated by emerging dislocations (*A*, *B*, and *C*) are clearly visible in Fig. 1(a). The crucial point is that the terrace splitting produces strong inhomogeneous strain distribution within the T_2 terrace. The whole T_2 terrace remains, in fact, only slightly strained, its elastic relaxation reveals a well-known (2×1)-O strip phase[14,15] dominating the surface [Fig. 1(b)]. By contrast, the small surface areas ($<1\times10^{-3}$ ML depending on the actual stress distribution) in close vicinity to the emerging dislocations become highly strained due to the strong local lattice deformation imposed by the dislocation geometry. This extra strain perturbed locally the dominating (2×1)-O strip phase causing its transformation into strikingly different phases, denoted as *A* and *B* in Fig. 1(b). The suggestion on the crucial role of the surface strain is supported by lateral asymmetry of these phases with respect to the corresponding dislocations. These phases were always located on the low-lying subterraces strained compressively [Fig. 1(b)] and were never observed on the high-lying subterraces where tensile strain was developed. In order to further confirm this suggestion, the extra strain was quantitatively estimated by analyzing the corresponding vertical lattice deformation. Curvatures of the Cu substrate in close vicinity of each dislocation were deduced from corresponding STM height profiles [Fig. 1(d)] and compared with that of the relaxed T_2 terrace. The striking observation is that the amount of the produced phases correlates reasonably well with the surface curvatures of the corresponding low-lying terraces [Fig. 1(c)]. The larger extra strain was, the larger surface area was occupied by the corresponding phase. The absence of such phases around *C* dislocation, where the extra strain is the smallest among the three dislocations, is remarkable. It indicates that there is a strain threshold below which these phases are not stable. Far from the dislocations, the relaxed T_2 terrace is deformed only slightly, its residual strain is close to the zero strain of an ideally flat surface [Fig. 1(c)], the relaxed (2×1)-O strip phase dominates the terrace. In order to further elaborate the role of the extra strain in the phases formation we will consider in details one of the produced phases, namely phase *A*, whose structure is shown in details in Fig. 2. In our study we paid special attention to the state of the STM tip. The surface was first scanned a sufficiently long time until "trapping" of an O atom by the STM tip, typically occurring on Cu(110)-(2×1)-O surfaces,[16] was detected. Height profiles taken on the (2×1)-O phase confirmed[16] the O-type character of the STM tip. The "O tip" visualized Cu atoms only[16,17] that allowed us to identify the white protrusions on all the STM topographies as Cu atoms composing the A_1, A_2, and (2×1)-O phases. These Cu atoms are apparently bonded to adsorbed oxygen (not visible on the STM topographies). Separation of the Cu-O units would produce low-coordinated Cu atoms that are known to be very unstable on surfaces.[18] The tendency of the Cu-O units to gather into long continuous Cu-O chains, which can be arranged into different configurations on the Cu(110) surface [e.g., (2×1)-O and $c(6\times2)$-O phases], has been well-established.[12,17] This allowed us to interpret the structure of the A_1 phase [Fig. 2(b)], as continuous zigzag Cu-O chains running in the [001] direction [Fig. 2(e)]. The registry of this structural model with respect to the Cu substrate was determined by its matching to the known structure of the (2×1)-O phase [Fig. 2(d)]. It can be immediately realized that these zigzag chains closely resemble the straight Cu-O chains forming the (2×1)-O phase, where the Cu atoms have been laterally displaced by an external force.

Now we will demonstrate that this correlation between the A_1 and the (2×1)-O phases is physically meaningful and determined by the dislocation-induced extra strain. More-

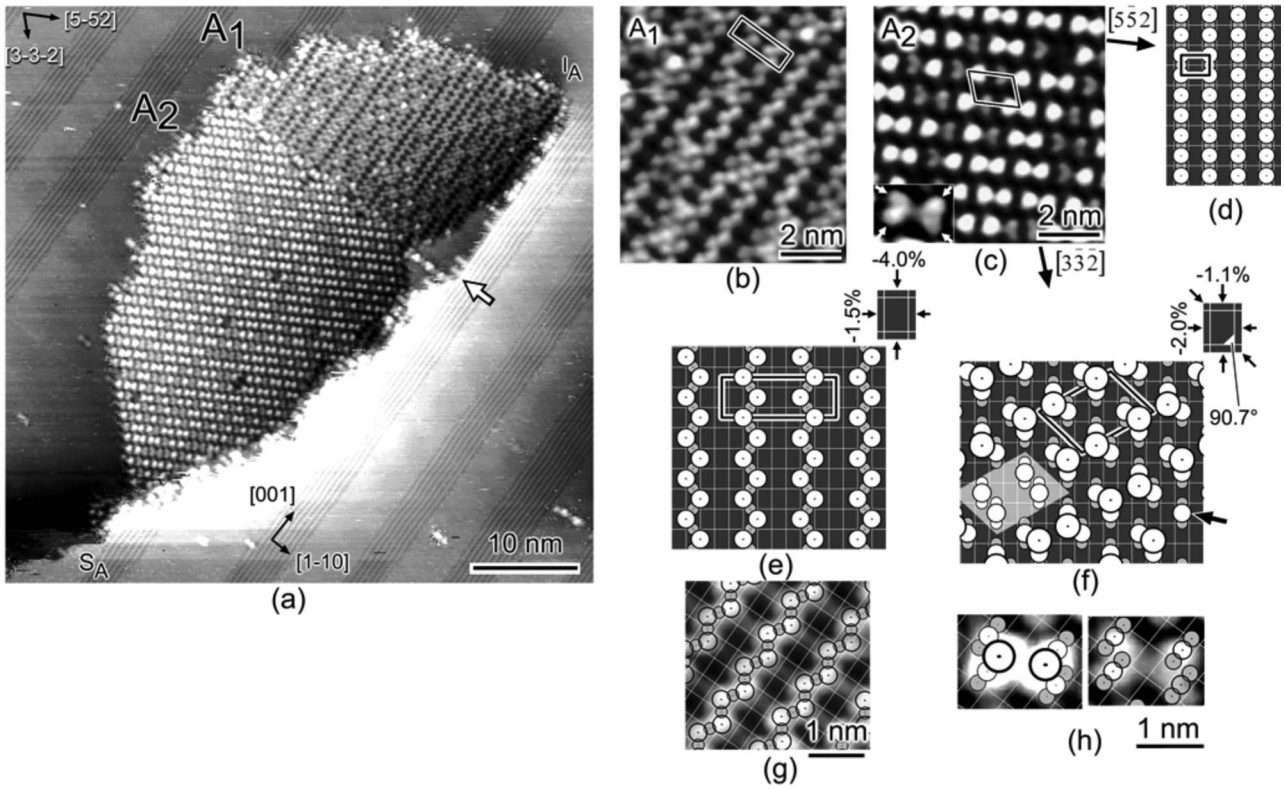

FIG. 2. Structural analysis of the A phase. (a) STM topography of the A phase. Two distinct phases, A_1 and A_2, constituting the A phase are marked consequently. (b) STM topography of the A_1 phase. The chains are regularly spaced in the $[1\bar{1}0]$ direction with the $\times 4$ periodicity, the $\times 1$ shift of each second chain in the [001] direction reveals the $c(8\times 2)$ unit cell which is specified by the black-and-white lines. (c) STM topography of the A_2 phase: a two-dimensional array of Cu-O clusters ordered in the $[5\bar{5}2]$ and $[3\bar{3}\bar{2}]$ directions, the corresponding $[\frac{5}{2}\frac{2}{2}]$ unit cell is specified. In inset: the single cluster containing four Cu atoms (marked by arrows). The bright roundlike protrusions are the Cu adatoms randomly adsorbed on top of the clusters and screening their characteristic butterflylike shape. (d) Schematics of the (2×1)-O phase. The white grid lines represent the close-packed rows of the Cu substrate. The O and Cu atoms of the (2×1)-O phase are shown as gray and white circles, respectively. The (2×1) unit cell is specified by the black-and-white lines. (e)–(f) Structural models of the (e) A_1 phase and (f) A_2 phase. The Cu adatoms on (f) are shown as white circles of larger size, the O-Cu-O chain fragment is marked by arrow, the Cu_4O_8 cluster is highlighted. The strain of the Cu lattice underlying the A_1 and A_2 phases is shown schematically at the upper-right corner of each model. The arrows designate the strain direction, the values represent the compression of the Cu lattice (in percents to the nominal lattice parameter) measured in the [001] and $[1\bar{1}0]$ directions. (g)–(h) Matching the structural models, shown on (e) and (f), with the corresponding STM topographies, shown in (b) and (c).

over, formation of both A_1 and A_2 phases can be explained reasonably well in terms of lateral evolution of the extra strain on the surface. All the phases observed in this study—A_1, A_2 and (2×1)-O—are reconstructed commensuratively with the Cu substrate. This allowed us to obtain quantitative information on the stress compressing the underlying subterraces. The predetermined symmetry of the A_1 and A_2 phases made possible to measure the (1×1) unit cell of the Cu lattice underlying each phase. The relative compression of the Cu lattice was then deduced taking the (2×1)-O phase as a reference; the results are shown in Figs. 2(e) and 2(f). Now the correlation between the A_1 and (2×1)-O phases becomes clear. The 4% compression of the low-lying subterrace, induced by the extra strain, resulted in equivalent compression of the (2×1)-O chains. The Cu atoms are displaced out of the "squeezed" chains in attempt to accommodate the shortening Cu-O bond length [Fig. 2(e)]. The increased repulsion between the chains[19] stabilizes the less dense equidistant (4×1) configuration of the zigzag Cu-O chains [Fig. 2(e)] revealing the A_1 phase. It is interesting to note that the lateral spreading of the A_1 phase around the I_A point is in qualitative agreement with the evolution of the extra strain on the surface. When going away from the dislocation, the extra strain dissipates very rapidly due to its local character. Thus, the semicircular interface between the A_1 and the (2×1)-O phases, in fact, bounds the surface area outside of which the residual strain no longer stabilized the zigzag structure, the Cu-O chains maintained their original (2×1)-O configuration [Fig. 2(a)]. The remarkable observation is, however, the formation of the A_2 phase [Fig. 2(c)]. Such as in the case of the A_1 phase, the semicircular phase boundary is also established accommodating the dissipating extra strain. However, no more chains of any kind have been detected neither inside the A_2 phase nor on the adjacent surface area [Fig. 2(a)]. This phase consists of a two-dimensional array of atomic scale clusters ordered in the $[5\bar{5}2]$ and $[3\bar{3}\bar{2}]$ directions. The absence of chains is surprising because of the well-known tendency for mobile Cu-O

units to be assembled into continuous (2×1)-O chains.[12,17] We will show in the following that the reason of the coexistence of the two differently reconstructed A_1 and A_2 phases is a specific directional character of the extra strain. As it can be seen in Figs. 1(a) and 1(b), the A dislocation, splitting the T_2 terrace into two subterraces, introduced the S_A surface step. This surface step, starting at I_A, initially propagates in the [001] direction being essentially parallel to the (2×1)-O chains [Fig. 2(a)]. This propagation does not perturb the orthogonality of the Cu lattice, the stress in the [001] direction compressed the straight (2×1)-O chains into the zigzag configuration. The situation, however, changes qualitatively ~20 nm away from the I_A point along the propagating step. Despite of the fact that the extra strain dissipates gradually as suggested the direct measurements of the (1×1) unit-cell compression [Figs. 2(e) and 2(f)], an additional strain component appears. Starting from the particular point [marked by the arrow in Fig. 2(a)], the S_A step deviates progressively from its initial direction and propagates toward the T_2 terrace edge finally joining it [Fig. 1(a)]. This deviation induced additional compression but now in direction imposed by the step orientation which neither coincides with [001] nor $[1\bar{1}0]$ directions. This situation should break the orthogonality of the adjacent Cu substrate and this nonorthogonality has been detected. Thorough analysis of the A_2 topography reveals the nonorthogonal (1×1) unit cell with the angle deviating by 0.7° from its reference value of 90° [Fig. 2(f)]. The relaxation of this nonorthogonal compression of the Cu substrate was then clearly detected as slight nonparallelism of the Cu-O chains belonging to the high- and low-lying subterraces (not shown). The observed Cu lattice nonorthogonality is proposed to play a decisive role in breaking the continuous Cu-O chains. Starting from the deviation point the chains accommodated the progressively developed nonorthogonality by self-fragmentation [Fig. 2(a)]. The abrupt A_1/A_2 phase boundary is, therefore, established almost coinciding with the deviation point. The produced O-Cu-O fragments remained, however, straight [the highlighted area in Fig. 2(f)], the reduced 1.1% compression of the Cu lattice no longer stabilized the strained zigzag configuration. The produced fragments were paired and then rearranged into the ordered array of the Cu_4O_8 clusters forming the A_2 phase [Figs. 2(c) and 2(f)]. The registry of this model with respect to the Cu substrate was determined by matching the A_2 structure with the previously determined A_1 structure. The proposed model also explains the origin of the Cu adatoms of the A_2 phase. The fragmentation of the (2×1)-O chains (the Cu-O ratio is 1:1) into the Cu_4O_8 clusters (Cu:O=1:2) implies that half of the Cu atoms have been expulsed from the chains. The expulsed atoms diffused thermally out of the A_2 phase, but some of them have been adsorbed on top of the O-Cu-O fragments as it shown schematically in Fig. 2(f) giving rise to the single- and double-occupied Cu_4O_8 clusters visible in Fig. 2(c).

In conclusion, we have reported the first direct experimental evidence that extra strain introduced into a surface can modify locally the state of chemisorbed particles and fabricate particularly reconstructed phases. The structural models of the discovered A_1 and A_2 phases account well for all the characteristics of the observed STM topographies [Figs. 2(g) and 2(h)]. The proposed models are consistent with evolution of the extra strain on the surface as well as the well-studied reactivity of the Cu-O chains. We hope that the observed strain-driven creation of these phases will bring further insight in understanding of thermodynamic properties of strained surfaces.

[1] H. Ibach, Surf. Sci. Rep. **29**, 195 (1997).
[2] C. Klink, L. Olesen, F. Besenbacher, I. Stensgaard, E. Laegsgaard, and N. D. Lang, Phys. Rev. Lett. **71**, 4350 (1993).
[3] K. Pohl, M. C. Bartelt, J. de la Figuera, N. C. Bartelt, J. Hrbek, and R. Q. Hwang, Nature (London) **397**, 238 (1999).
[4] M. Mavrikakis, B. Hammer, and J. K. Nørskov, Phys. Rev. Lett. **81**, 2819 (1998).
[5] D. Sander, C. Schmidthals, A. Enders, and J. Kirschner, Phys. Rev. B **57**, 1406 (1998).
[6] A. Schlapka, M. Lischka, A. Gross, U. Krasberger, and P. Jakob, Phys. Rev. Lett. **91**, 016101 (2003).
[7] F. Calleja, V. M. Garcia-Suarez, J. J. Hinarejos, J. Ferrer, A. L. Vasquez de Parga, and R. Miranda, Phys. Rev. B **71**, 125412 (2005).
[8] S. Narasimhan, Phys. Rev. B **69**, 045425 (2004).
[9] M. Gsell, P. Jacob, and D. Menzel, Science **280**, 717 (1998).
[10] N. Reinecke, S. Reiter, S. Vetter, and E. Taglauer, Appl. Phys. A: Mater. Sci. Process. **75**, 1 (2002).
[11] D. J. Coulman, J. Wintterlin, R. J. Behm, and G. Ertl, Phys. Rev. Lett. **64**, 1761 (1990).
[12] N. Hartmann and R. J. Madix, Surf. Sci. **488**, 107 (2001).
[13] H.-C. Jeong and E. D. Williams, Surf. Sci. Rep. **34**, 171 (1999).
[14] K. Kern, H. Niehus, A. Schatz, P. Zeppenfeld, J. Goerge, and G. Comsa, Phys. Rev. Lett. **67**, 855 (1991).
[15] Ch. Bombis, M. Moiseeva, and H. Ibach, Phys. Rev. B **72**, 245408 (2005).
[16] L. Ruan, F. Besenbacher, I. Stensgaard, and E. Laegsgaard, Phys. Rev. Lett. **70**, 4079 (1993).
[17] R. Feidenhans'l, F. Grey, M. Nielsen, F. Besenbacher, F. Jensen, E. Laegsgaard, I. Stensgaard, K. W. Jacobsen, J. K. Norskov, and R. L. Johnson, Phys. Rev. Lett. **65**, 2027 (1990).
[18] K. W. Jacobsen and J. K. Nørskov, Phys. Rev. Lett. **65**, 1788 (1990).
[19] J. Harl and G. Kresse, Surf. Sci. **600**, 4633 (2006).